



# Long-term effect of plastic feeding on growth and transcriptomic response of mealworms (*Tenebrio molitor* L.)

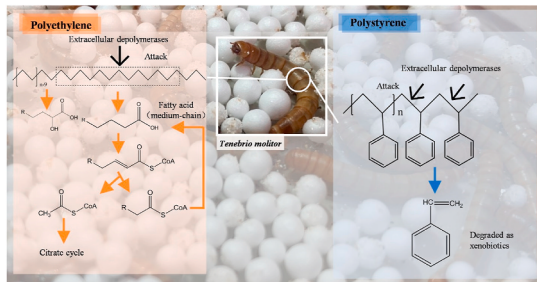
Zheng Zhong, Wenyang Nong, Yichun Xie, Jerome Ho Lam Hui, Lee Man Chu\*

School of Life Sciences, The Chinese University of Hong Kong, Shatin, NT, Hong Kong SAR, China

## HIGHLIGHTS

- We studied effects of plastics on mealworm growth and its mechanism in PS and PE degradation by transcriptomic analysis.
- Plastic consumption was negatively dependent on plastic crystallinity.
- Fatty acid degradation pathway was important in the digestion of plastic degradation intermediates.
- Depolymerases probably act on the distal backbone and produce shorter linear chains that containing  $\leq 16$  C atoms.
- Intermediates of PS degradation were further decomposed by mealworms as xenobiotics.

## GRAPHICAL ABSTRACT



## ARTICLE INFO

Handling Editor: Michael Bank

### Keywords:

Polystyrene  
Polyethylene  
Plastic degradation  
Biodegradative pathway  
Transcriptomics  
Fatty acid degradation pathway

## ABSTRACT

Plastic waste has been considered a serious global environmental problem for decades. Despite the high recalcitrance of synthetic plastics, the biodegradation of polyethylene (PE), polystyrene (PS), polypropylene (PP), and polyvinyl chloride (PVC) by some insect larvae has been reported; however, the mechanism of degradation remains largely unknown. We investigated the effects of plastics on the growth of mealworms (larvae of *Tenebrio molitor*) and their role in PS and PE degradation. Mealworms were capable of ingesting high-impact polystyrene (HIPS), expanded polystyrene (EPS) and low-density polyethylene (LDPE) but not linear low-density polyethylene (LLDPE) or polypropylene (PP). Plastic consumption was negatively dependent on plastic crystallinity. Transcriptome analysis and KEGG mapping revealed that mealworms act as downstream decomposers in plastic depolymerization and that fatty acid degradation pathways may play important roles in the digestion of plastic degradation intermediates produced by gut bacteria. In addition, PS and PE degradation was achieved via the diffusion of extracellular depolymerases, which probably acted on the distal backbone and produce shorter linear chains that containing  $\leq 16$  C atoms instead of branched chains. Additionally, the intermediates of PS degradation are expected to be further decomposed by mealworms as xenobiotics. This study provided a preliminary understanding of plastic degradation mechanism by mealworms.

\* Corresponding author.

E-mail address: [leemanchu@cuhk.edu.hk](mailto:leemanchu@cuhk.edu.hk) (L.M. Chu).

## 1. Introduction

Worldwide plastic production was reported to be 368 million tonnes in 2019 (PlasticsEurope, 2020), and 400 million tonnes of thermoplastics were produced globally in 2020 (Tiseo, 2021a). The major non-hydrolysable plastics include polyethylene (PE), polypropylene (PP), polystyrene (PS) and polyvinyl chloride (PVC), based on their production worldwide in 2018 (Tiseo, 2021b), i.e. PE, 32%; PP, 23%; PVC, 16% and PS, 7%. This enormous plastic production has imposed an immense burden in terms of waste management since polyolefins are largely nonbiodegradable.

Degrading recalcitrant plastics using insects has become a trendy topic globally. Gerhardt and Lindgren (1954) reported the ability of 9 species of common stored-product insects (*Tenebroides mauritanicus*, *Tribolium confusum*, *Stegobium paniceum*, *Blattella germanica*, *Sitophilus granaries*, *Plodia interpunctella*, *Rhyzopertha dominica*, *Ephestia kuhniella* and *Sitophilus oryzae*) to penetrate PE films. Holes and scratches in PP, PE and polyester films produced by adults of *R. dominica* and *S. oryzae* have been observed under scanning electron microscopy (Riuadavets et al., 2007). Two bacterial strains, *Enterobacter asburiae* YT1 and *Bacillus* sp. YP1, isolated from waxworm gut, were shown to achieve PE film degradation rates of 6.1% and 10.7% in their suspension cultures ( $10^8$  cells  $\text{mL}^{-1}$ ), respectively (Yang et al., 2014).

Mealworms (larvae of *Tenebrio molitor*) have been found to degrade expanded PS, PE, PP, PVC and polyactic acid (PLA) to lower-molecular-weight products, even  $\text{CO}_2$  (Brandon et al., 2018; Peng et al., 2020b, 2021; Yang et al., 2015, 2021a, 2021b). Degradation capabilities of expanded PS, PE, PP and rigid PS, PE, PVC by mealworm were evaluated by changes in number-, weight-, and size-average molecular weight ( $M_n$ ,  $M_w$  and  $M_z$ ) and functional groups by comparison of the feedstock and the residual polymer in collected frass. When considering non-microplastics, limited extent depolymerization pattern (reduction in either  $M_w$  or  $M_n$  or none after ingestion) was reported in the degradation of LDPE foam and PP foam (Yang et al., 2021a, 2021b, 2021b), while broad depolymerization pattern (reduction in both  $M_w$  and  $M_n$  after ingestion) occurred in EPS, LDPE and PVC (Brandon et al., 2018; Peng et al., 2019, 2020b; Yang et al., 2015a, 2018, 2021a). However, Wu et al. (2019) observed limited extent depolymerization pattern in mealworms fed with microplastics (PS, PVC and LDPE). Different behaviors in degradation imply that particle size, form and density of plastics greatly affect the degradation ability of mealworm.

To date, besides *T. molitor*, six insects (*Achroia grisella*, *Tenebrio obscurus*, *Zophobas atratus*, *Plesiophthalmus davidis*, *Plodia interpunctella* and *Galleria mellonella*) have been reported to have the ability to break down and modify the backbone of PS, PE, PVC and PP to some extent by either depolymerization pattern (Brandon et al., 2018; Kundungal et al., 2019; Luo et al., 2020; Peng et al., 2019, 2020a, 2020a; Woo et al., 2020). Different patterns in degradation of various plastics implied the complexity of degradation mechanism by larvae of these insects. Studies focused on the degradation of rigid plastics and the influence of plastics and plastic properties on the mealworms were limited. Due to the large production and the physicochemical properties differences in PP, PE and PS, in the present study, the degradation behavior of rigid plastic products, including low-density PE (LDPE), linear low-density PE (LLDPE), high-impact PS (HIPS, with rubber as additive) and PP, by mealworms was investigated, and expanded PS (EPS) was included for comparison. Yang et al. (2015b) suppressed the activities of gut bacteria in mealworms by antibiotics and observed great depression of PS degradation after treatment, implying the essential role of gut bacteria in PS degradation. Here, the mechanism of PS and PE degradation by mealworms was studied by RNA sequencing, which is a powerful approach for whole-transcriptome analysis, and via the expression analysis of differentially expressed genes (DEGs) with next-generation sequencing technology to measure transcript and isoform levels (Wang et al., 2020). Potentially relevant metabolic pathways and functional enzymes were identified by comparing DEGs between mealworms fed

either plastics (PS and PE) and wheat bran. The findings of this study provide a preliminary understanding of plastic degradation mechanism by mealworms.

## 2. Materials and methods

### 2.1. Plastic test materials

To assess the influence of the physicochemical properties of plastics on the survival and growth of mealworms, LDPE, LLDPE, EPS, HIPS and PP were purchased from SINOPEC (China) and EyeIslet (China). EPS was used as delivered (spherical, 2–3 mm), while the other materials were cut into 2–3 mm fragments. The materials were cleaned with compressed air prior to their use in mealworm rearing. Molecular weights ( $M_n$  and  $M_w$ ) and polydispersity index (PDI) of PP, LDPE and LLDPE were determined by high-temperature gel permeation chromatography (HT-GPC) via Agilent PL-GPC 220 coupled with refractive index detector, while those of EPS and HIPS by gel permeation chromatography (GPC) via Agilent 1260 coupled with 1100 refractive index detector, according to methods by Brandon et al. (2018). Density and shore hardness (HD) were determined at the Institute of Analysis, Guangdong Academy of Sciences (China National Analytical Center, Guangzhou, China). Polymer crystallinity was determined via differential scanning calorimetry by normalizing the observed heat of fusion to that of a 100% crystalline sample of the same polymer. For PE and PP, 293 and 209 J  $\text{g}^{-1}$  were selected as reference values of heat of fusion for the 100% crystalline sample (Kong and Hay, 2002; Kostoski and Stojanović, 1995). The properties of the plastics used are shown in Table 1.

### 2.2. Mealworm cultivation and plastic consumption

Mealworms (larvae of *T. molitor*) were provided by the Urban Protein Engineering Technology Research Center, which obtained the original insect colony from South China Agricultural University. Prior to the experiment, the mealworms were fed wheat bran (Bob's Red Mill, Milwaukee, USA). Before being fed the experimental diets, the mealworms were subjected to a 48-h starvation period (Yang et al., 2015a) and were then reared with the selected diets in 300 mL glass containers in a controlled-environment chamber (MGC-350HP, Yi Heng, Shanghai, China) under stable conditions (25 °C, 70% RH, in dark).

The worms were fed five experimental diets: LDPE, LLDPE, EPS, HIPS and PP, either alone or cofed with bran (1:1 w/w); unfed worms and worms fed on wheat bran were included as starvation and feeding controls, respectively. Each glass container contained 50 larvae of similar weight (~80 mg ind $^{-1}$ , ~3-month-old) and 3 g of the experimental plastics, bran or mixtures thereof (bran/plastics, 1/1), except in the starvation control, which received no diet. In the cofed diets, half of the required amount of bran based on the average weight of the worms was added every 5 days. All treatments were carried out with four replicates.

**Table 1**  
Properties of the studied plastics.

Plastics	Shore hardness (HD)	Density (g $\text{cm}^{-3}$ )	Crystallinity (%)	$M_n$ (kDa)	$M_w$ (kDa)	PDI
PP	$24.8 \pm 0.4$	$0.961 \pm 0.001$	8.53	70	244	3.54
LLDPE	$22.8 \pm 0.4$	$0.942 \pm 0.001$	3.91	31	103	3.32
LDPE	$24.0 \pm 0.0$	$1.015 \pm 0.006$	3.45	22	92	4.20
HIPS	$25.6 \pm 0.5$	$1.114 \pm 0.002$	Amorphous	67	164	2.49
EPS <sup>a</sup>	nd	<0.1	Amorphous	141	243	1.93

<sup>a</sup> Manufacturer's information; nd = no data.

To assess plastic degradation, frass of LDPE- and EPS-fed mealworm were collected after 14 days of experiment. Collected frass or plastic feedstock (50 mg) were freeze-dried for 48 h and stored under  $-20^{\circ}\text{C}$  before analysis. Molecular weight ( $M_w$  and  $M_n$ ) and PDI of LDPE and EPS were quantified by HT-GPC and GPC, respectively. Modification on functional groups was assessed by Fourier Transform Infrared Spectroscopy (FTIR) on Agilent Cary 630 FTIR, recorded in the range of 4000–500  $\text{cm}^{-1}$ . All treatments were carried out with two replicates. Larvae were removed immediately after death. Survived larvae or pupae were counted and weighed, and residual plastics were weighed. The development and growth status of the mealworms were evaluated according to their mortality (%) and relative weight of larvae (%).

The biodegradability of the tested plastics was assessed according to their cumulative consumption ( $\text{mg ind}^{-1}$ ), which was computed as the accumulation of the weight of plastics consumed (mg) per surviving larva every 5 days until all studied larvae were dead.

### 2.3. RNA extraction and Illumina sequencing

To assess the PS and PE degradation mechanisms, three mealworms ( $\sim 80 \text{ mg ind}^{-1}$ ,  $\sim 3$ -month-old) fed EPS, LDPE and wheat bran for 2, 3 and 4 weeks were prepared for RNA extraction (totally 27 larvae). After washing with deionized water and ethanol, larval whole RNA was extracted using TRIzol reagent (Ambion, Austin, TX, USA) according to the manufacturer's instructions. The quality and quantity of RNA were assessed via gel electrophoresis (1% agarose gels) and with a Nanodrop spectrophotometer (Thermo Fisher Scientific). Transcriptome sequencing was performed by Novogene (Hong Kong).

### 2.4. Transcriptome analysis

Raw sequencing reads from the transcriptomes were preprocessed via quality trimming by Trimmomatic (v0.33 with parameters “ILLUMINACLIP:TruSeq3-PE.fa:2:30:10 SLIDINGWINDOW:4:5 LEADING:5 TRAILING:5 MINLEN:25”) (Bolger et al., 2014), followed by *de novo* transcriptome assembly using Trinity (v2.9.1) (Grabherr et al., 2011; Haas et al., 2013) with the options “–SS lib type RF –normalize\_reads” and other default parameters. All biological duplicates were combined to carry out the *de novo* assembly and estimation of transcript abundance using the “align\_and\_estimate\_abundance.pl” script of Trinity software with “–est\_method RSEM –aln\_method bowtie2” (v2.4.2) (Langmead, 2010). Coding regions within transcripts were annotated using TransDecoder (v5.0.2) (Haas et al., 2013), and functional annotations and analyses were carried out using Trinotate (v3.1.1, Haas).

Differential expressed genes (DEGs) between mealworms fed on traditional food (wheat bran) and plastics (EPS and LDPE) were visualized with Degust (v4.1.1, Powell) (edgeR (Robinson et al., 2010), false discovery rate (FDR)  $\leq 0.05$ ,  $|\log_2(\text{foldchange})| \geq 1$ , minCPM  $\geq 50$  in at least 1 sample). To further assign predicted gene descriptions, the assembled sequences of the DEGs were compared to the proteins in the National Center for Biotechnology Information (NCBI) Nr database with the BLASTX algorithm according to the threshold of an E-value  $< 10^{-5}$ . Kyoto Encyclopedia of Genes and Genomes (KEGG) annotation and pathway mapping for each DEG were performed using Blast2GO (version 5.2.5) software (Conesa et al., 2005).

Annotation of functional term in Gene Ontology (GO) enrichment analysis was performed using eggNOG (Huerta-Cepas et al., 2018) with default parameters and taxon restricted to Metazoa (Taxon ID:33208). Genes were assigned with GO terms. Functional enrichment of DEGs was tested using function ‘compareCluster()’ in R package ‘clusterProfiler’ v.3.16.1 (Yu et al., 2012) under the environment of R 4.1.0 (R Core Team, 2021). Significantly enriched terms were determined with adjusted pvalueCutoff = 0.20, pAdjustMethod = “BH”. Data were visualized using R packages ‘ggplot2’ (Wickham, 2016).

The raw reads generated in this study have been deposited to the NCBI database under the BioProject accessions: PRJNA687344

(information is listed in Table S1).

### 2.5. Real-time PCR (RT-PCR) validation

cDNA synthesis was performed using a reverse transcription kit (PrimeScript RT Master Mix, Takara Bio Inc, Shiga, Japan) following the manufacturer's protocol. Primers for the RT-PCR analysis of identical target genes were designed by using Primer3Plus (<http://www.bioinformatics.nl/cgi-bin/primer3plus/primer3plus.cgi>) and are listed in Supplementary Table S2. RT-PCR was performed with half iTaq<sup>TM</sup> Universal SYBR<sup>®</sup> Green Supermix (BioRad) on a CFX96 Touch<sup>TM</sup> Real-Time PCR Detection System (BioRad) according to the manufacturer's manual. The program for RT-PCR was as follows: 95 °C for 3 min for denaturation, followed by 40 cycles of 95 °C for 10 s, 55 °C for 10 s and 72 °C for 15 s. Three biological replicates were performed for each gene detected by RT-PCR, with TmL27a employed as the housekeeping gene (Jang et al., 2020).

### 2.6. Statistical analysis

Interactive plots were generated using R packages “ggplot2” (Wickham, 2016), “plotly” (Sievert, 2020) and “htmlwidgets” (Vaidyanathan et al., 2020) under the environment of R 4.1.0 (R Core Team, 2021).

The obtained data were processed using SPSS (IBM SPSS Statistics 17). One-way analysis of variance (ANOVA) was used to analyze statistical significance ( $p < 0.05$ ). Tukey's post hoc test was used if equal variances were assumed, while the Games-Howell test was used if equal variances were not assumed. Pearson correlation and Spearman correlation were used to evaluate correlations between cumulative plastic consumption with molecular weight ( $M_n$  and  $M_w$ ) and crystallinity, respectively, since crystallinity is not a continuous variable.

## 3. Results and discussion

### 3.1. Evaluation of biodegradation and oxidation of EPS and LDPE

GPC analysis of the feedstock and residual polymer in collected frass revealed the changes of molecular weight, providing direct evidence of plastic depolymerization. For EPS,  $M_n$  and  $M_w$  were reduced 11.6% and 13.6%, respectively, while PDI increased from 1.92 to 2.37, indicating that mealworm had no discrimination on molecular weight in PS depolymerization. Besides, appearance of new carbonyl groups (1900–1600  $\text{cm}^{-1}$ ), broadening peaks of hydroxyl groups (3700–3100  $\text{cm}^{-1}$ ) and shift of peaks caused by methylene from 801  $\text{cm}^{-1}$  to 849  $\text{cm}^{-1}$  in the FTIR spectra (Fig. S1A) provided solid evidences of depolymerization. In contrast,  $M_n$  and  $M_w$  of LDPE increased 27.4% and 9.4% respectively after ingestion by mealworms, while PDI decreased from 4.20 to 3.66, implying that mealworms tended to attack the polymer with light molecular weight. Besides, oxidation of LPDE was proved by appearance of new peaks in the FTIR spectra (Fig. S1B) associated with hydroxyl group stretching (3700–3100  $\text{cm}^{-1}$ ), carbonyl group stretching (1900–1600  $\text{cm}^{-1}$ ) and C–O stretching (1200–1000  $\text{cm}^{-1}$ ). These results provided additional evidences of depolymerization and oxidation of EPS and LDPE after ingestion by mealworms, but in different patterns, i.e. EPS, broad depolymerization pattern and LDPE, limited extent depolymerization pattern.

### 3.2. Plastic consumption by mealworms

The cumulative consumption (Fig. 1A and B) of HIPS, EPS and LDPE with or without bran increased throughout the experimental period, while that of LLDPE and PP remained unchanged. For better visualize each treatment and comparison, inactive plots ([https://github.com/xieyichun50/Plastic\\_Tenebrio\\_molitor](https://github.com/xieyichun50/Plastic_Tenebrio_molitor)) were supplied. The addition of bran greatly improved both the ingestion of plastics and the growth of the mealworms. Under the same circumstances, the consumption of

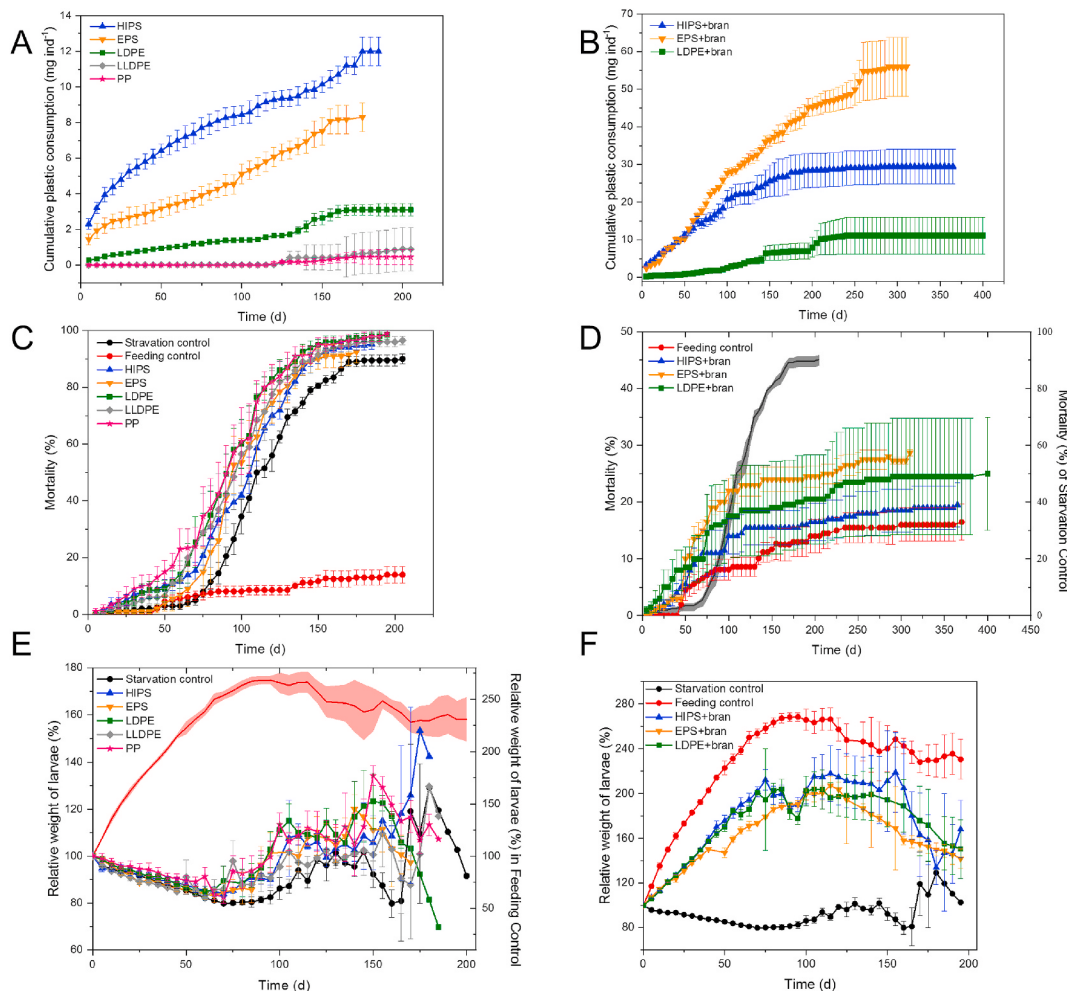


**Fig. 1.** Cumulative plastic consumption ( $\text{mg ind}^{-1}$ ) of plastic-fed groups (A) and bran cofed groups (B) over time, mortality (%) of plastic-fed groups (C) and bran cofed groups (D) over time (line with gray shading represents the mortality of starvation control using the right y axis and sharing the same x axis with other groups), and relative larval weight (%) of plastic-fed groups (E) and bran cofed groups (F) from 5 to 200 d, (line with red shading represents the relative weight of starvation control using the right y axis and sharing the same x axis with others). Vertical bars are the standard errors of four replicates. (For interpretation of the references to colour in this figure legend, the reader is referred to the Web version of this article.)

HIPS and EPS was significantly greater than that of the other plastics with or without bran addition ( $p < 0.05$ ). The consumption of PS alone was even higher than that of LDPE + bran. Moreover, when fed with bran, cumulative plastic consumption of PP and LLDPE in 30 d were only 0.09 and 0.32  $\text{mg ind}^{-1}$ , respectively, which were six and two times lower than LDPE + bran (0.57  $\text{mg ind}^{-1}$ ). Data collection ended since little plastics were consumed.

LDPE (linear chain with branching) and LLDPE (linear chain with less branching compared with LDPE) were products of PE with different chemical structures. Although the hardness and density of LLDPE were lower than those of LDPE (Table 1), mealworm preferred LDPE, implying that hardness and density were not the key factors in plastic degradation by mealworm. Besides, there were no significant correlations between molecular weight and consumption (*i.e.*  $M_n$ : Pearson  $r = 0.492$ ,  $p > 0.05$ ;  $M_w$ : Pearson  $r = 0.194$ ,  $p > 0.05$ ). Within the plastic-fed groups, cumulative consumption was negatively dependent on crystallinity (Spearman  $r = -0.975$ ,  $p = 0.005 < 0.01$ ). The highest cumulative consumption was observed in HIPS, an amorphous polymer, while the lowest was observed in PP which had the highest crystallinity (8.53%). It has been reported that crystallinity decreases the degradability of poly(ethylene terephthalate) by *Ideonella sakaiensis* (Yoshida et al., 2016). The spontaneous diffusion of extracellular depolymerase results in the preferential degradation of the amorphous region to crystalline lamellae. Yang et al. (2018) found that PS consumption had strong

negative correlations with density, though our findings suggested that crystallinity was more important as a factor on plastic consumption by mealworm.

Compared with PE and PS, there is a paucity of studies on the biodegradation of PP which is more crystalline, although it is one of the most widely used plastics in the world. In our study, rigid PP was not consumable while Yang et al. (2021b) found that mealworm performed limited extent depolymerization on the degradation of PP foam. Unlike PE and PS, manufacturing of expanded PP (EPP) requires stricter conditions because of the highly crystalline structure. Additives such as  $\text{NaHCO}_3$  and azodicarbonamide are indispensable in its production. The unclear physicochemical properties and the additives in the PP foam used made it difficult for comparison, although either PP foam or rigid PP was semicrystalline. In our study, HIPS and EPS are rigid and foamy respectively, though both are amorphous structures. In the absence of bran, the cumulative consumption of HIPS and EPS was similar ( $p = 0.689 > 0.05$ ), while the consumption of EPS with bran was almost twice as high as that of HIPS with bran. When the same weight of PS was placed in the containers, there was a higher probability of larvae accessing EPS than HIPS. In the case of PP and EPP, besides crystallinity, feeding density and accessibility could be other important factors that influence their consumption.

### 3.3. Long-term effects on mealworm growth

The mortality of the mealworms fed on the different diets was examined until all larvae died or pupated. In the worms that were fed only plastics, mortality (Fig. 1C and D) significantly increased. The highest mortality of the groups cofed with bran was observed for EPS + bran, followed by LDPE + bran, HIPS + bran and feeding control. The mortality rates of the groups that were fed plastics alone showed the following descending order: PP (99.0%), LDPE (98.5%), LLDPE (96.0%), HIPS (95.2%), EPS (92.5%), starvation control (90.0%). HIPS and EPS, which have similar chemical backbones, had different effects on the survival of mealworms. Despite showing the highest ingestion rate, EPS had a negative effect on growth. The ability of mealworms to use PS as the sole C source was limited. The energy released by digesting PS does not account for the energy spent on nutrition. This result was not in accord with previous research (Brandon et al., 2018) but provided additional information to evaluate the potential of plastic degradation by insects.

The relative weights of the larvae (Fig. 1E and F) that fed on bran with or without plastics all increased steadily to a peak at 100–130 d, followed by a slow decline towards the end of the experiment. In contrast, the relative weights of larvae from the starvation control group and treatments involving plastics alone decreased slowly until approximately 65 d, followed by an increase and then a sharp decline at the end of the experiment (Fig. 1E). The apparent increases in the relative weights of the worms in the middle of the experimental period were largely attributed to the death of the weaker larvae. The remaining larvae were greater and stronger, and exhibited a relatively higher biomass. Considering the lack of food in these groups and the cannibalistic behavior of mealworms, the larvae were likely to attack each other and survived by eating their companions. In the absence of food, the surviving larvae still suffered from starvation, which finally led to a decline in their weight until they died. The relative weights of the larvae in the HIPS, EPS, LDPE, LLDPE and PP groups at the lowest point in their initial decline were similar to those in the starvation control group. The amount of plastics consumed by the mealworms corresponded to a very small proportion of the weight of larvae. Therefore, the ingested plastics contributed insignificantly to the growth of larvae, which finally resulted in a reduction in larval weight. Although the mealworms could degrade PS and PE, they failed to grow by feeding on plastics alone.

Except the influences on larval weight, plastic feeding affected pupation with shorter development time (larvae fed with plastics pupated when grown to ~50% weight of the bran fed groups). Peng et al. (2021) observed that sole PLA diet accelerated the pupation of mealworm but led to failure in becoming adult. Further research should be conducted to elucidate the underlying factors and mechanisms involved.

### 3.4. Transcriptome analysis of mealworms fed with LDPE and EPS

Compared with the feeding control, a total of 307 and 413 sequences (samples collected after 2, 3 and 4 weeks) showed significant changes after feeding on EPS and LDPE, respectively. After annotation, 28 and 60 DEGs were matched as uncharacterized proteins, while 74 and 77 DEGs from each group showed no matches in the database, which may result from insufficient reference transcriptome data. Eriksson et al. (2020) published the 312 Mb draft reference genome of *T. molitor* with 16,090 genes being annotated. However, due to the shortage of genome resources when the study was carried out, *de novo* transcriptome assembly results were presented.

The number of downregulated DEGs was almost two times greater than the number of upregulated ones (Fig. 2A, S2, and S3). Hydrolases had the greatest changes in all classes of enzymes based on enzyme-catalyzed reactions (Fig. 2B). Focusing on the group fed with LDPE, in the case of lacking nutrition, upregulations were observed in hydrolases acting on ester bonds (*i.e.* 2w, phosphatidylinositide phosphatase SAC2; 3w, esterase FE4, phospholipase D2; 4w, type I inositol 1,4,5-

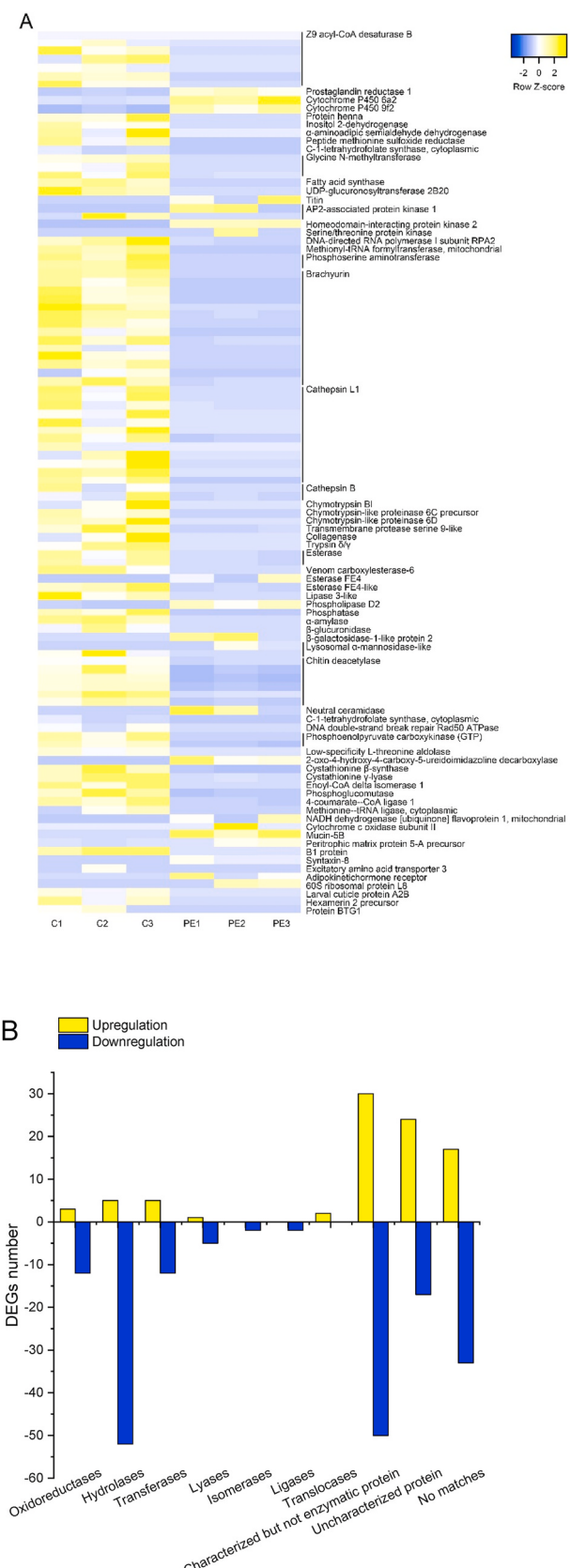


**Fig. 2.** Heatmap (C: feeding control; PE: mealworm fed with LDPE) (A) and distribution ( $n_{\text{total DEGs}} = 271$ ,  $n_{\text{(downregulated DEGs}}} = 185$ ,  $n_{\text{(upregulated DEGs}}} = 86$ ) (B) of DEGs identified in the bran- and LDPE-fed groups after 3 weeks.

trisphosphate 5-phosphatase), sugars (*i.e.* 2w, myrosinase 1, glycoprotein endo-alpha-1,2-mannosidase; 3w, lysosomal  $\alpha$ -mannosidase-like protein,  $\beta$ -galactosidase-1-like protein 2; 4w,  $\beta$ -galactosidase-1-like protein 2), and C–N bonds (3w, neutral ceramidase), probably producing long-chain alcohols, long-chain C–C or C–N linked carboxylates, or long-chain fatty acids from LDPE. Detailed information of DEGs encoding oxidoreductases, hydrolases and lyases are listed in Table S3. GO enrichment analysis of LDPE-fed group (Fig. S4) showed that activities related to fatty acid metabolic process (biological process) were expanded.

For EPS-fed groups, cleavages on sugars (2w, lysosomal  $\alpha$ -mannosidase-like precursor), peptide bonds (*i.e.* 2w, brachyurin; 3w, brachyurin, modular serine protease zymogen, aminopeptidase N-like protein, mitochondrial respiratory chain complex I assembly), and acid anhydrides (3w, developmentally-regulated GTP-binding protein 2 and eukaryotic initiation factor 4A-III) were increased, which were more related to energy supply (ATP-dependent reactions). For GO enrichment analysis, no significantly enriched terms were shown in EPS group.

According to the KEGG mapping results, the DEGs of the mealworms fed on EPS and LDPE were significantly enriched in 42 and 39 specific pathways, respectively (Table S4). In the worms that fed on either plastic, the KEGG pathway analysis of DEGs indicated that fatty acid degradation and isoniazid metabolism (drug metabolism - other enzymes) were involved in the breakdown of PS and PE. The simplified pathways with all DEGs are shown in Figs. 3A and 4A. To validate the RNA-Seq data, all DEGs involved in these pathways were selected for RT-PCR analysis in the plastic- and bran-fed mealworms.

### 3.5. Fatty acid degradation

Fatty acid degradation, which mostly occurs in mitochondria, is the process in which fatty acids are broken down and results in the removal of 2-C units from the carboxyl terminus of acyl-CoA to produce acetyl-CoA. The key enzymes involved in this process are acyl-CoA oxidase (EC 1.3.3.6, 1.3.8.7, 1.3.8.1), enoyl-CoA hydratase (EC 4.2.1.17), 3-hydroxyacyl-CoA dehydrogenase (EC 1.1.1.35, 1.1.1.21), and acetyl-

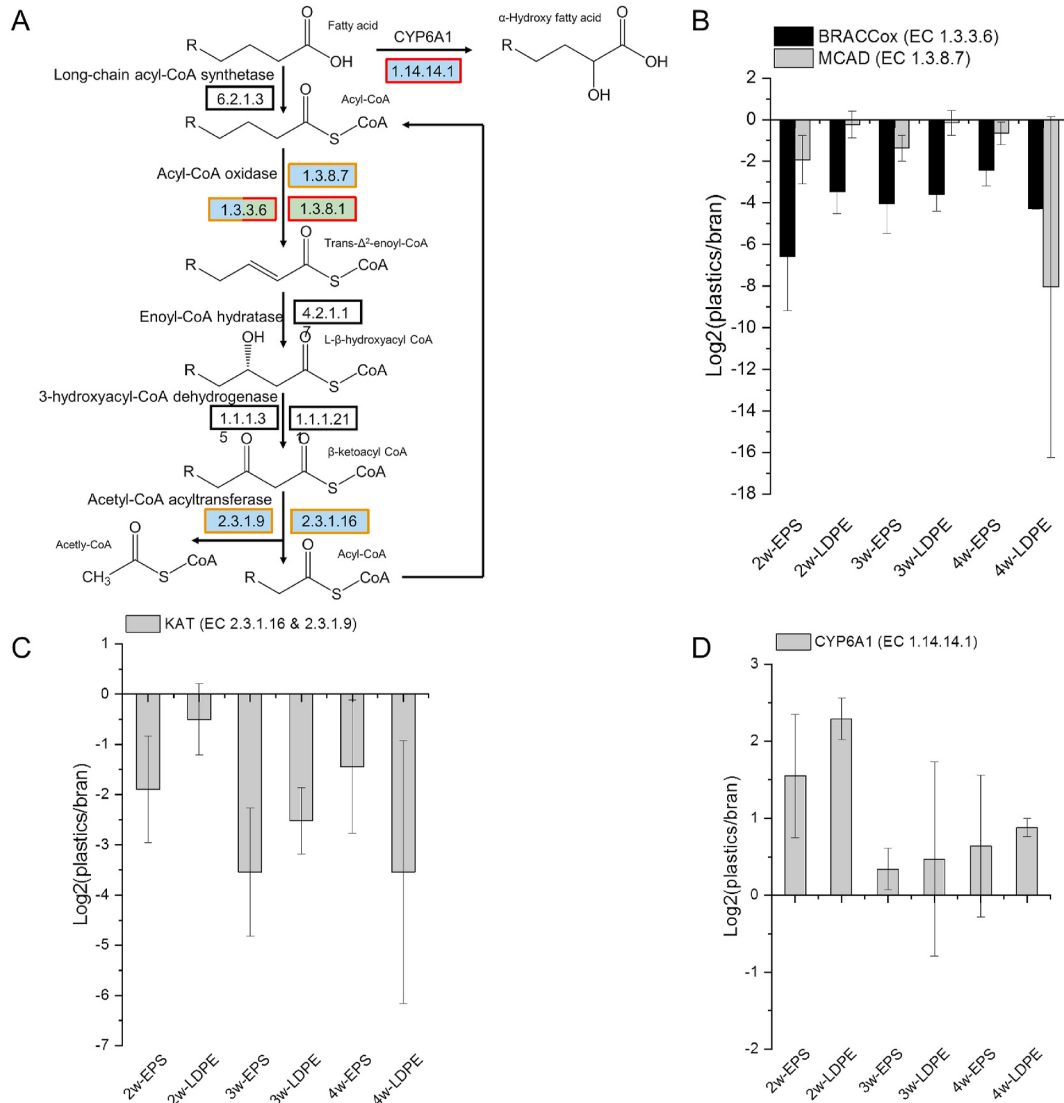


**Fig. 3.** DEGs related to fatty acid degradation in bran- and plastic-fed mealworms. A. Simplified fatty acid degradation pathway. A red box indicates the DEGs showing upregulation relative to feeding control; a yellow box indicates the DEGs that were downregulated; a half red and half yellow box indicates that some of the sequences were upregulated while others were downregulated. The DEGs with green shading belong to the EPS-fed group, while those with blue shading belong to the LDPE-fed group. Non-change genes are marked with black borders. B – D. RT-PCR validation of the expression levels of acyl-CoA (EC 1.3.3.6, 1.3.8.7), acetyl-CoA acyltransferase (EC 2.3.1.16, 2.3.1.9) and cytochrome P450 6A1 (EC 1.14.14.1). (For interpretation of the references to colour in this figure legend, the reader is referred to the Web version of this article.)

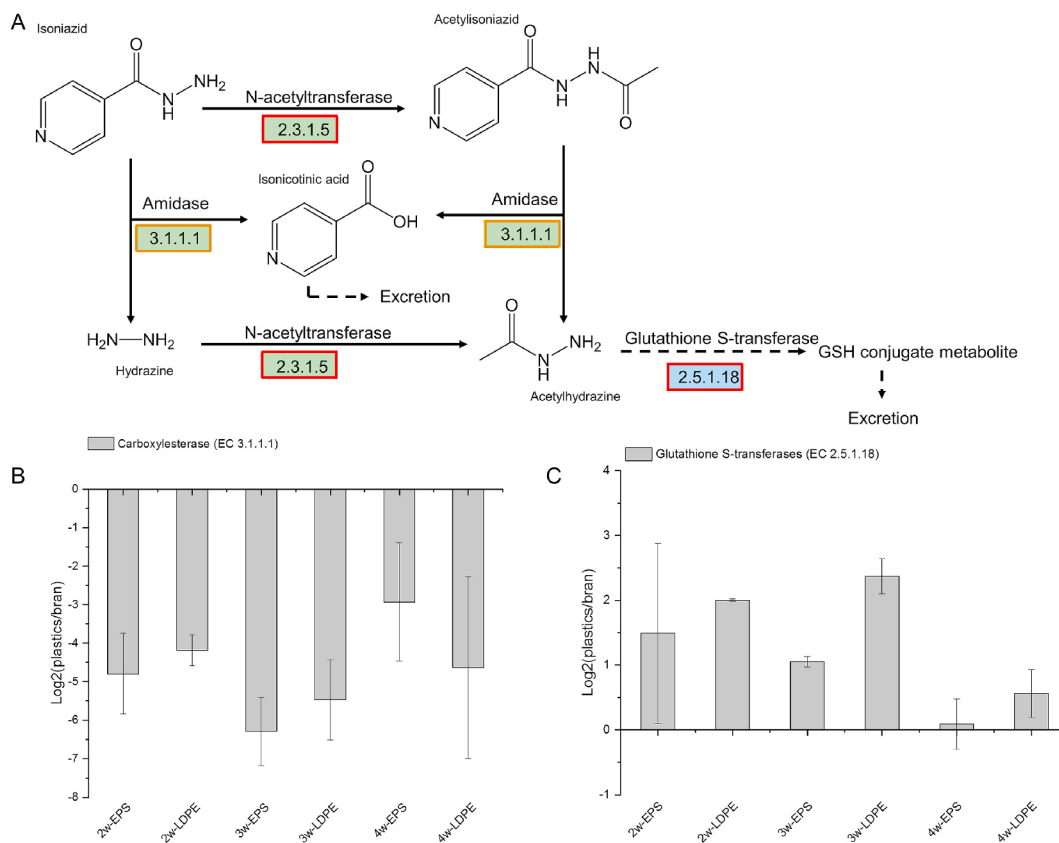


**Fig. 4.** DEGs between bran- and plastics-fed mealworms related to drug (isoniazid) metabolism. A. Simplified isoniazid metabolism pathway. A red box indicates DEGs that were upregulated relative to feeding control; a yellow box indicates DEGs that were downregulated. DEGs with green shading belong to the EPS-fed group, while those with blue shading belong to the LDPE-fed group. Dashed arrows indicate more than one step of reactions are involved. B and C. RT-PCR validation of the expression levels of carboxylesterase (EC 3.1.1.1) and glutathione S-transferases (EC: 2.5.1.18), respectively. (For interpretation of the references to colour in this figure legend, the reader is referred to the Web version of this article.)

CoA acyltransferase (EC 2.3.1.16, 2.3.1.19). The Degust results for the pathway-related DEGs are listed in Table S5.

In this pathway, the RT-PCR-based expression patterns of medium chain specific acyl-CoA (MCAD, EC 1.3.8.7), peroxisomal acyl-CoA oxidase 3 (BRACCOX, EC 1.3.3.6), 3-ketoacyl-CoA thiolase (KAT, EC 2.3.1.16, 2.3.1.19), and cytochrome P450 6A1 (CYP6A1, EC 1.14.14.1) were consistent with the transcriptome analysis (Fig. 3B-D). Acyl-CoA oxidases include several enzymes that can be sorted according to the different lengths of their target chains. Among the identified DEGs, MCAD shows specificity for chain lengths of 4–16, while BRACCOX oxidizes the CoA esters of 2-methyl-branched fatty acids. Both BRACCOX and MCAD were suppressed in the worms fed on plastics alone. Except for the DEGs identified in the 4w-LDPE group (Fig. 3B), the suppression of BRACCOX was greater than that of MCAD. Because of the lack of nutrition, activities related to the energy supply, growth and development were probably suppressed. The weaker suppression of MCAD indicated that the production of medium-chain fatty acids was greater than that of branched fatty acids in plastic-fed mealworms. Due to manufacturing differences, the linear backbone of LDPE, is equipped with both long and short branched chains, while PS has a linear backbone with benzene ring side groups. The greater downregulation of BRACCOX indicated that extracellular depolymerases probably secreted by gut bacteria (Yang et al., 2015b; Yoshida et al., 2016) shall act on the distal backbone and produce shorter linear chains containing less than 16 C atoms instead of branched chains.

KAT, which functions in the downstream reaction in the pathway, was downregulated probably due to the suppression of MCAD and BRACCOX.

CYP6A1 inserts oxygen atoms into fatty acids with chain lengths of

12–18 C atoms (Farinas et al., 2001). The overexpression of CYP6A1 in the plastic-fed groups provided evidence of the depolymerization mechanism whereby more fatty acids containing 12–18 C atoms were formed in plastic-fed mealworms than in bran-fed mealworms. In addition to CYP6A1, two other DEGs from the LDPE-fed and bran-fed groups were annotated as members of the cytochrome P450s: CYP6A2 and CPY9F2, respectively (Table S3), which showed increased expression.

These findings were consistent with previous research (LeMoine et al., 2020), suggesting that alcohol dehydrogenase and aldehyde dehydrogenase (oxidizing alcohols into aldehydes and carboxylates) were overexpressed, compared with starvation and honeycomb-fed control in *G. mellonella* larvae. Besides, Kong et al. (2019) evaluated the transcriptomic responses on long-chain fatty acid metabolism on *G. mellonella* larvae fed with and without beeswax which is common in hydrocarbon chains with PE. They revealed that genes related to carboxylesterase and lipase 1 and 3 families were overexpressed in the groups fed on beeswax. Moreover, expression levels of gene families related to short-chain fatty acid degradation and carbon, methane and propanoate metabolism were upregulated in gut tissues from *G. mellonella* larvae fed on beeswax, while lipases and cytochromes potentially related to wax degradation was decreased, suggesting that intestinal microbiota were inclined to decompose short-chain fatty acids produced from wax degradation by larvae. This finding was inconsistent with the report on mealworm, indicating that gut bacteria play crucial roles in plastic degradation, as their depression inhibit the depolymerization of PE, PS, PP and PVC (Brandon et al., 2018; Peng et al., 2020b; Yang et al., 2015b, 2021b). Although larvae of *G. mellonella* and *T. molitor* showed differences in plastic degradation, pathway related to

fatty acid metabolism was involved in both species.

### 3.6. Isoniazid metabolism

Acetylation and hydrolysis are the major metabolic reactions to which isoniazid is subjected and are mediated by n-acetyltransferase (NAT, EC 2.3.1.5) and carboxylesterase (CES, EC 3.1.1.1), respectively. NAT catalyzes the acetylation of aryl amines from acetyl-CoA. Carboxylesterase 2 (CES2) belongs to a class of enzymes that hydrolyze carboxylic esters and usually exhibit amide-related activities. They are of great importance in the metabolism of drugs and xenobiotics and were among the DEGs identified in PS-fed mealworms. The causes of the decrease in CES2 expression at 3 weeks (Fig. 4B) were numerous and unclear. It has been reported that oysterol and fatty acids, metabolites of the CES catalytic reaction, both act as inhibitors of CES in humans (Xu et al., 2016). Yang et al. (2015a) reported that the <sup>13</sup>C values of fatty acids were significantly higher in mealworms fed <sup>13</sup>C-labeled PS than in worms fed bran, especially unsaturated fatty acids. The production of fatty acids, especially unsaturated fatty acids, may suppress the expression of CES in mealworms.

Glutathione S-transferases (GSTs, EC 2.5.1.18) constitute a multi-gene family of Phase II metabolic isozymes that are involved in detoxification. The upregulation of GSTs (Fig. 4C) in the plastic-fed groups indicated that the degradation intermediates may have negative effects on mealworms since they are treated as xenobiotics. By feeding the worms only plastics, a portion of the energy released from plastic degradation is used in the detoxification of breakdown intermediates. This finding agrees with the results regarding the effects on the growth of mealworms described previously.

Hexameric rings (pyridine and benzene) are similar in structure to isoniazid and styrene, the monomers of PS. We hypothesized that extracellular depolymerases catalyze the depolymerization of the distal backbone of PS, periodically producing modified monomers. The products are continuously acetylated, hydrolyzed and conjugated by NAT, CES2 and GSTs, respectively, similar to the metabolism of isoniazid. Since the genome resource of *T. molitor* was released on NCBI in May 2021 (Eriksson et al., 2020), the reconstruction of transcriptome by genome-guided assembly is indispensable to obtain the comprehensive set of recovered transcripts. More research is needed to validate the hypothesis.

## 4. Conclusions

Mealworms were capable of ingesting HIPS, EPS and LDPE, but not LLDPE and rigid PP. This work provides the first description of the long-term effects of plastics on the growth of mealworms. Plastic consumption, which contributed very little to the growth of larvae, was negatively dependent on plastic crystallinity. Additional nutrition was essential for mealworm survival, and mealworm failed to survive and grow by feeding on plastics alone. Our findings suggested that the degradation of plastics was caused by the diffusion of extracellular depolymerases that acted on the distal polymer backbone and produced shorter linear chains containing  $\leq 16$  C atoms instead of branched chains. The intermediates of PS degradation are treated as xenobiotics by mealworms.

## Credit author statement

Zheng Zhong: Investigation, Methodology, Writing – original draft preparation, Validation, Formal analysis, Software; Wenyang Nong: Data curation, Formal analysis, Software; Yichun Xie: Writing – review & editing, Data curation, Formal analysis, Software; Jerome Ho Lam Hui: Supervision, Methodology, Resources, Writing – review & editing; Lee Man Chu\*: Supervision, Methodology, Writing – review & editing, Resources, Conceptualization, Funding acquisition, Project administration.

## Declaration of competing interest

The authors declare that they have no known competing financial interests or personal relationships that could have appeared to influence the work reported in this paper.

## Acknowledgments

We thank all members of our laboratory for their valuable advice on the project and manuscript. We also appreciate the technical support provided by Dr. Xi Zhou, Institute of Analysis, Guangdong Academy of Sciences (China National Analytical Center, Guangzhou).

## Appendix A. Supplementary data

Supplementary data to this article can be found online at <https://doi.org/10.1016/j.chemosphere.2021.132063>.

## Abbreviation description

ANOVA	analysis of variance
BRACCOx	peroxisomal acyl-CoA oxidase 3
CES	carboxylesterase
CPY	cytochrome P450
CPY6A1	cytochrome P450 6A1
DEG	differentially expressed gene
EPS	expanded polystyrene
FDR	false discovery rate
FTIR	Fourier transform infrared spectroscopy
GPC	gel permeation chromatography
GSTs	glutathione s-transferases
GO	gene ontology
HT-GPC	high-temperature gel permeation chromatography
HIPS	high-impact polystyrene
KAT	3-ketoacyl-CoA thiolase
KEGG	Kyoto Encyclopedia of Genes and Genomes
LDPE	low-density polyethylene
LLDPE	linear low-density polyethylene
MCAD	medium chain specific acyl-CoA
NAT	n-acetyltransferase
NCBI	National Center for Biotechnology Information
PDI	polydispersity index
PE	polyethylene
PLA	polyactic acid
PP	polypropylene
PS	polystyrene
PVC	polyvinyl chloride
RT-PCR	real-time polymerase chain reaction

## References

- Bolger, A.M., Lohse, M., Usadel, B., 2014. Trimmomatic: a flexible trimmer for Illumina sequence data. Bioinformatics 30, 2114–2120. <https://doi.org/10.1093/bioinformatics/btu170>.
- Brandon, A.M., Gao, S.-H., Tian, R., Ning, D., Yang, S.-S., Zhou, J., Wu, W.-M., Criddle, C. S., 2018. Biodegradation of polyethylene and plastic mixtures in mealworms (Larvae of *Tenebrio molitor*) and effects on the gut microbiome. Environ. Sci. Technol. 52, 6526–6533. <https://doi.org/10.1021/acs.est.8b02301>.
- Conesa, A., Götz, S., García-Gómez, J.M., Terol, J., Talón, M., Robles, M., 2005. Blast2GO: a universal tool for annotation, visualization and analysis in functional genomics research. Bioinformatics 21, 3674–3676. <https://doi.org/10.1093/bioinformatics/bti610>.
- Eriksson, T., Andere, A.A., Kelstrup, H., Emery, V.J., Picard, C.J., 2020. The yellow mealworm (*Tenebrio molitor*) genome: a resource for the emerging insects as food and feed industry. J. Insects as Food Feed 6 (5), 445–455. <https://doi.org/10.3920/JIFF2019.0057>.
- Farinas, E.T., Schwaneberg, U., Glieder, A., Arnold, F.H., 2001. Directed evolution of a cytochrome P450 monooxygenase for alkane oxidation. Adv. Synth. Catal. 343, 601–606. [https://doi.org/10.1002/1615-4169\(200108\)343:6<601::AID-ADSC601>3.0.CO;2-9](https://doi.org/10.1002/1615-4169(200108)343:6<601::AID-ADSC601>3.0.CO;2-9).

- Gerhardt, P.D., Lindgren, D.L., 1954. Penetration of various packaging films by common stored-product insects. *J. Econ. Entomol.* 47, 282–287. <https://doi.org/10.1093/jee/47.2.282>.
- Grabherr, M.G., Haas, B.J., Yassour, M., Levin, J.Z., Thompson, D.A., Amit, I., Adiconis, X., Fan, L., Raychowdhury, R., Zeng, Q., Chen, Z., Mauceli, E., Hacohen, N., Gnirke, A., Rhind, N., di Palma, F., Birren, B.W., Nusbaum, C., Lindblad-Toh, K., Friedman, N., Regev, A., 2011. Full-length transcriptome assembly from RNA-Seq data without a reference genome. *Nat. Biotechnol.* 29, 644–652. <https://doi.org/10.1038/nbt.1883>.
- Haas, B.J. Trinotate: transcriptome functional annotation and analysis. <https://github.com/Trinotate/Trinotate.github.io/wiki>.
- Haas, B.J., Papanicolaou, A., Yassour, M., Grabherr, M., Blood, P.D., Bowden, J., Couger, M.B., Eccles, D., Li, B., Lieber, M., MacManes, M.D., Ott, M., Orvis, J., Pochet, N., Strozzi, F., Weeks, N., Westerman, R., William, T., Dewey, C.N., Henschel, R., LeDuc, R.D., Friedman, N., Regev, A., 2013. *De novo* transcript sequence reconstruction from RNA-seq using the Trinity platform for reference generation and analysis. *Nat. Protoc.* 8, 1494–1512. <https://doi.org/10.1038/nprot.2013.084>.
- Huerta-Cepas, J., Szklarczyk, D., Heller, D., Hernández-Plaza, A., Forslund, S.K., Cook, H., Mende, D.R., Letinic, I., Rattei, T., Jensen, L.J., Mering, C.V., Bork, P., 2018. eggNOG 5.0: a hierarchical, functionally and phylogenetically annotated orthology resource based on 5090 organisms and 2502 viruses. *Nucleic Acids Res.* 47, 309–314. <https://doi.org/10.1093/nar/gky1085>.
- Jang, H.A., Park, K.B., Kim, B.B., Ali Mohammadi Kojour, M., Bae, Y.M., Baliarsingh, S., Lee, Y.S., Han, Y.S., Jo, Y.H., 2020. Bacterial but not fungal challenge up-regulates the transcription of *Coleoptericin* genes in *Tenebrio molitor*. *Entomol. Res.* 50, 440–449. <https://doi.org/10.1111/1748-5967.12465>.
- Kong, Y., Hay, J.N., 2002. The measurement of the crystallinity of polymers by DSC. *Polymer* 43, 3873–3878. [https://doi.org/10.1016/S0032-3861\(02\)00235-5](https://doi.org/10.1016/S0032-3861(02)00235-5).
- Kong, H.G., Kim, H.H., Chung, J., Jun, J., Lee, S., Kim, H., Jeon, S., Park, S.G., Bhak, J., Ryu, C., 2019. The *Galleria mellonella* hologenome supports microbiota-independent metabolism of long-chain hydrocarbon beeswax. *Cell Rep.* 26, 2451–2464. <https://doi.org/10.1016/j.celrep.2019.02.018>.
- Kostoski, D., Stojanović, Ž., 1995. Radiation-induced crystallinity changes and melting behavior of drawn isotactic polypropylene. *Polym. Degrad. Stabil.* 47, 353–356. [https://doi.org/10.1016/0141-3910\(94\)00126-X](https://doi.org/10.1016/0141-3910(94)00126-X).
- Kundungal, H., Gangarapu, M., Sarangapani, S., Patchaiyappan, A., Devipriya, S.P., 2019. Efficient biodegradation of polyethylene (HDPE) waste by the plastic-eating lesser waxworm (*Achroia grisella*). *Environ. Sci. Pollut. Res.* 26, 18509–18519. <https://doi.org/10.1007/s11356-019-05038-9>.
- Langmead, B., 2010. Aligning short sequencing reads with Bowtie. *Curr. Protoc. Bioinformatics* 32, 11–17. <https://doi.org/10.1002/0471250953.bi1107s32>.
- LeMoine, C.M.R., Grove, H.C., Smith, C.M., Cassone, B.J., 2020. A very hungry caterpillar: polyethylene metabolism and lipid homeostasis in larvae of the greater wax moth (*Galleria mellonella*). *Environ. Sci. Technol.* 54, 14706–14715. <https://doi.org/10.1021/acs.est.0c04386>.
- Lou, Y., Ekaterina, P., Yang, S.-S., Lu, B., Liu, B., Ren, N., Corvini, P.F.-X., Xing, D., 2020. Biodegradation of polyethylene and polystyrene by greater wax moth larvae (*Galleria mellonella* L.) and the effect of co-diet supplementation on the core gut microbiome. *Environ. Sci. Technol.* 54, 2821–2831. <https://doi.org/10.1021/acs.est.9b07044>.
- Peng, B.-Y., Su, Y., Chen, Z., Chen, J., Zhou, X., Benbow, M.E., Criddle, C.S., Wu, W.-M., Zhang, Y., 2019. Biodegradation of polystyrene by dark (*Tenebrio obscurus*) and yellow (*Tenebrio molitor*) mealworms (Coleoptera: tenebrionidae). *Environ. Sci. Technol.* 53, 5256–5265. <https://doi.org/10.1021/acs.est.8b06963>.
- Peng, B.-Y., Li, Y., Fan, R., Chen, Z., Chen, J., Brandon, A.M., Criddle, C.S., Zhang, Y., Wu, W.-M., 2020a. Biodegradation of low-density polyethylene and polystyrene in superworms, larvae of *Zophobas atratus* (Coleoptera: tenebrionidae): broad and limited extent depolymerization. *Environ. Pollut.* 266, 115206. <https://doi.org/10.1016/j.envpol.2020.115206>.
- Peng, B.-Y., Chen, Z., Chen, J., Yu, H., Zhou, X., Criddle, C.S., Wu, W.-M., Zhang, Y., 2020b. Biodegradation of polyvinyl chloride (PVC) in *Tenebrio molitor* (Coleoptera: tenebrionidae) larvae. *Environ. Int.* 145, 106106. <https://doi.org/10.1016/j.envint.2020.106106>.
- Peng, B.-Y., Chen, Z., Chen, J., Zhou, X., Wu, W.-M., Zhang, Y., 2021. Biodegradation of polylactic acid by yellow mealworms (larvae of *Tenebrio molitor*) via resource recovery: a sustainable approach for waste management. *J. Hazard Mater.* 416, 125803. <https://doi.org/10.1016/j.jhazmat.2021.125803>.
- PlasticsEurope, 2020. Plastics – the facts 2020. <https://www.plasticseurope.org/en/re-sources/publications/4312-plastics-facts-2020>.
- Powell, D.R., 2019. Degust: Interactive RNA-Seq Analysis. <https://doi.org/10.5281/zendo.3258932>.
- R Core Team, 2021. R: a language and environment for statistical computing. Vienna, Austria. Retrieved from. <https://www.r-project.org/>.
- Riudavets, J., Salas, I., Pons, M.J., 2007. Damage characteristics produced by insect pests in packaging film. *J. Stored Prod. Res.* 43, 564–570. <https://doi.org/10.1016/j.jspr.2007.03.006>.
- Robinson, M.D., McCarthy, D.J., Smyth, G.K., 2010. edgeR: a Bioconductor package for differential expression analysis of digital gene expression data. *Bioinformatics* 26, 139–140. <https://doi.org/10.1093/bioinformatics/btp616>.
- Sievert, C., 2020. Interactive Web-Based Data Visualization with R, Plotly, and Shiny. Chapman and Hall/CRC Florida.
- Tiseo, L., 2021a. Global production volume of thermoplastics by type 2020-2050. <https://www.statista.com/statistics/1192886/thermoplastics-production-volume-by-type-globally/>.
- Tiseo, L., 2021b. Distribution of plastic production worldwide in 2018. by type. <https://www.statista.com/statistics/968808/distribution-of-global-plastic-production-by-type/>.
- Vaidyanathan, R., Xie, Y., Allaire, J.J., Cheng, J., Sievert, C., Russell, K., 2020. htmlwidgets: HTML Widgets for R. R package. version 1.5.3. <https://cran.r-project.org/packages=htmlwidgets>.
- Wang, H.-Z., Zhong, X., Zhang, G.-R., Liu, X., Gu, L., 2020. Transcriptome characterization and gene expression analysis related to immune response in *Gynaephora qinghaiensis* pupae. *J. Asia Pac. Entomol.* 23 (2), 458–469. <https://doi.org/10.1016/j.aspen.2020.01.013>.
- Wickham, H., 2016. ggplot2: Elegant Graphics for Data Analysis. Springer-Verlag, New York. Retrieved from. <https://ggplot2.tidyverse.org>.
- Woo, S., Song, I., Cha, H.J., 2020. Fast and facile biodegradation of polystyrene by the gut microbial flora of *Plesiophthalmus davidi* larvae. *Appl. Environ. Microbiol.* 86, e01361 <https://doi.org/10.1128/AEM.01361-20>.
- Wu, Q., Tao, H., Wong, M.H., 2019. Feeding and metabolism effects of three common microplastics on *Tenebrio molitor* L. *Environ. Geochem. Health* 41, 17–26. <https://doi.org/10.1007/s10653-018-0161-5>.
- Xu, Y., Zhang, C., He, W., Liu, D., 2016. Regulations of xenobiotics and endobiotics on carboxylesterases: a comprehensive review. *Eur. J. Drug Metab. Pharmacokinet.* 41, 321–330. <https://doi.org/10.1007/s13318-016-0326-5>.
- Yang, J., Yang, Y., Wu, W.-M., Zhao, J., Jiang, L., 2014. Evidence of polyethylene biodegradation by bacterial strains from the guts of plastic-eating waxworms. *Environ. Sci. Technol.* 48, 13776–13784. <https://doi.org/10.1021/es504038a>.
- Yang, Y., Yang, J., Wu, W.-M., Zhao, J., Song, Y., Gao, L., Yang, R., Jiang, L., 2015a. Biodegradation and mineralization of polystyrene by plastic-eating mealworms: part 1. chemical and physical characterization and isotopic tests. *Environ. Sci. Technol.* 49, 12080–12086. <https://doi.org/10.1021/acs.est.5b02661>.
- Yang, Y., Yang, J., Wu, W.-M., Zhao, J., Song, Y., Gao, L., Yang, R., Jiang, L., 2015b. Biodegradation and mineralization of polystyrene by plastic-eating mealworms: part 2. role of gut microorganisms. *Environ. Sci. Technol.* 49, 12087–12093. <https://doi.org/10.1021/acs.est.5b02663>.
- Yang, S.-S., Brandon, A.M., Flanagan, J.C.A., Yang, J., Ning, D., Cai, S.-Y., Fan, H.-Q., Wang, Z.-Y., Ren, J., Benbow, E., Ren, N.-Q., Waymouth, R.M., Zhou, J., Criddle, C. S., Wu, W.-M., 2018. Biodegradation of polystyrene wastes in yellow mealworms (larvae of *Tenebrio molitor* Linnaeus): factors affecting biodegradation rates and the ability of polystyrene-fed larvae to complete their life cycle. *Chemosphere* 191, 979–989. <https://doi.org/10.1016/j.chemosphere.2017.10.117>.
- Yang, L., Gao, J., Liu, Y., Zhuang, G., Peng, X., Wu, W.-M., Zhuang, X., 2021a. Biodegradation of expanded polystyrene and low-density polyethylene foams in larvae of *Tenebrio molitor* Linnaeus (Coleoptera: tenebrionidae): broad versus limited extent depolymerization and microbe-dependence versus independence. *Chemosphere* 262, 127818. <https://doi.org/10.1016/j.chemosphere.2020.127818>.
- Yang, S.-S., Ding, M.-Q., He, L., Zhang, C.-H., Li, Q.-X., Xing, D.-F., Cao, G.-L., Zhao, L., Ding, J., Ren, N.-Q., Wu, W.-M., 2021b. Biodegradation of polypropylene by yellow mealworms (*Tenebrio molitor*) and superworms (*Zophobas atratus*) via gut-microbe-dependent depolymerization. *Sci. Total Environ.* 756, 144087. <https://doi.org/10.1016/j.scitotenv.2020.144087>.
- Yoshida, S., Hiraga, K., Takehana, T., Taniguchi, I., Yamaji, H., Maeda, Y., Toyohara, K., Miyamoto, K., Kimura, Y., Oda, K., 2016. A bacterium that degrades and assimilates poly(ethylene terephthalate). *Science* 351, 1196–1199. <https://doi.org/10.1126/science.aad6359>.
- Yu, G., Wang, L.-G., Han, Y., He, Q.-Y., 2012. clusterProfiler: an R package for comparing biological themes among gene clusters. *OMICS* 16, 284–287. <https://doi.org/10.1089/omi.2011.0118>.